

Role of Adipose-Derived Stem Cells in Restoring Ovarian Structure of Adult Albino Rats with Chemotherapy-Induced Ovarian Failure: A Histological and Immunohistochemical Study

Faten Riad Omar¹, Noha Mohamed Afifi Amin^{1*}, Hala Ahmed Elsharif² and Dina Hisham Mohamed³

¹Professor of Histology, Faculty of Medicine, Cairo University, Cairo, Egypt

²Lecturer of Histology, Faculty of Medicine, Cairo University, Cairo, Egypt

³Demonstrator of Histology, Faculty of Medicine, Cairo University, Cairo, Egypt

*Corresponding author: Noha Mohamed Afifi Amin, Faculty of Medicine, Cairo University, 7 El-Tebarsy street, Kasr-Al-Aini street, Cairo, Egypt, Tel: 00201069626557; E-mail: noha_afifi@windowslive.com

Received date: January 19, 2016; Accepted date: February 11, 2016; Published date: February 13, 2016

Copyright: © 2016, Omar FR, et al. This is an open-access article distributed under the terms of the Creative Commons Attribution License, which permits unrestricted use, distribution, and reproduction in any medium, provided the original author and source are credited.

Abstract

Background and objectives: Damage to the reproductive system is one of the most devastating effects of chemotherapeutic treatment. It is frequently associated with premature ovarian failure (POF). Therefore, this study was planned to evaluate the therapeutic effectiveness of Adipose-Derived Stem Cells (ADSCs) in a rat model of chemotherapy-induced ovarian failure.

Methods and results: This study was carried out on forty adult female albino rats. They were divided into: Group I Control Group (n=8) received a vehicle of phosphate buffered saline (PBS) solution. Group II in which ovarian failure (OF) was induced using combined cyclophosphamide/busulfan therapy and were sacrificed after one week (gIIa n=8) and after five weeks (gIIb n=8). Group III in which rats received ADSCs after chemotherapy and were sacrificed after one week (gIIIa n=8) and after four weeks (gIIIb n=8). Blood samples were analysed for serum estradiol, FSH & LH. Ovarian sections were subjected to H&E, Masson's Trichrome and immunohistochemical staining for anti-PCNA antibody. The mean number of primordial follicles, mean area % of collagen fibers, mean area % of +ve immunoreactivity for PCNA were measured by histomorphometric studies and statistically compared. ADSCs proved to have a therapeutic potential in improving ovarian structure and function following chemotherapy, evidenced at both the morphological and laboratory level.

Conclusions: The greatest effect of ADSCs was achieved after the longer duration of therapy which lasted for four weeks.

Keywords: Premature ovarian failure; Chemotherapy; Adipose derived stem cells; PCNA

Introduction

Anticancer drugs are unquestionably beneficial as therapeutic agents. However, their side effects on the quality of life of female cancer survivors and their off springs cannot be ignored. One of the most devastating effects of chemotherapy is damage to the reproductive system, which in young girls and women younger than forty years of age is frequently associated with premature ovarian failure (POF) [1].

Restoration of reproductive function following chemotherapy is of increasing importance given that survival rates are improving. Currently, there are no proven treatments that restore fertility potential or even normal functionality to a woman's ovaries after chemotherapeutic treatment [2].

One of the most common therapeutic strategies for women with POF is hormone replacement therapy (HRT), however, HRT has been shown to increase the risk of blood clots in the veins as well as ovarian and breast cancer [3].

Over the past three decades, Bone Marrow Stem Cells (BMSCs) have been used as a popular cell source for regenerative medicine

research. However, the isolation of BMSCs frequently yields a low number of stem cells and the isolation procedure is invasive for donors and patients [4].

Concerning the application of Embryonic Stem Cells (ESCs), these have many disadvantages including tumorigenicity and ethical considerations [5].

In contrast, adipose tissue has recently been identified as one of the alternative sources of multipotent resident stem cells in humans. Adipose-derived stem cells (ADSCs) are a new type of MSCs that are typically abundant in individuals. They comprise a type of multipotent adult stem cells isolated from adipose tissue [6].

The biologic characteristics of ADSCs resemble those of adult stem cells from marrow. However, adipose tissue represents an abundant, poorly immunogenic, stably proliferative, low-injury and practical tissue source that holds great promise for autologous cell repair and regeneration [7].

The present study was designed to test the therapeutic potential of ADSCs in improving ovarian structure and folliculogenesis in a rat model of combined cyclophosphamide-busulfan induced ovarian failure, monitored by histological, immunohistochemical and morphometric methods.

Material and Methods

Material

(I) Drugs

a) **Cyclophosphamide (CY) (Trade name Endoxan):** It was purchased from Baxter Oncology GmbH, Halle, Germany, in the form of a vial 200 mg. The drug was dissolved in 10ml phosphate buffered saline (PBS) solution. Rats were injected intraperitoneal (I.P) with a single dose, 120 mg/kg [8].

b) **Busulfan (Trade name Myleran):** The drug was purchased from Excella GmbH, Nurnberger, Germany, in the form of tablets 2 mg. Tablets were crushed and dissolved in phosphate buffered saline (PBS) solution. It was given orally by the use of a special blunt tipped syringe, at a dose of 30 mg/kg, single dose [8].

(II) Animals

The study was conducted at the Animal House of Kasr Al Ainy School of Medicine, according to the guidelines for the Care and Use of Laboratory Animals. Forty adult female albino rats (12 weeks old) were used in this experiment, their weights ranged from 180-200 (185 ± 1.25) gram. They were fed ad libitum and allowed free access to water.

They were divided into the following groups:

Group I (GI) Control Group included 8 rats that were subdivided into:

gIa: 4 rats received 0.5 ml PBS (solvent of CP & busulfan) by intraperitoneal (I.P) injection as well as oral route.

gIb: 4 rats received the same regimen as in subgroup Ia, then received 0.5 ml PBS (solvent of stem cells) by intravenous (I.V.) route through rat tail vein.

- Rats were sacrificed with the corresponding experimental subgroups.
- **Group II (GII)** included 16 rats in which ovarian failure (OF) was induced using combined cyclophosphamide/busulfan therapy. It was subdivided into:

gIIa: 8 rats were sacrificed 1 week after chemotherapy to confirm ovarian failure.

gIIb: 8 rats were left untreated and were sacrificed 5 weeks after chemotherapy to assess spontaneous recovery from chemotherapy treatment.

- **Group III (GIII)** included 16 rats in which ovarian failure was induced by the same regimen as in group II. After 1 week of chemotherapeutic treatment, the animals received 2 million units of PKH-labeled ADSCs/ animal I.V. through tail vein, single dose. It was subdivided into:

IIIa: 8 rats were sacrificed 1 week after the ADSCs injection.

IIIb: 8 rats were sacrificed 4 weeks after the ADSCs injection.

Methods

Induction of ovarian failure [*combined cyclophosphamide/busulfan therapy*]

Cyclophosphamide was solubilized in PBS solution. The solution was prepared and injected I.P. within 15 minutes of its preparation, at a dose of 120 mg/kg. Busulfan was dissolved in PBS solution and given concomitantly with cyclophosphamide, orally at a dose of 30 mg/kg, single dose [8]. This was performed at the Histology Department, Faculty of Medicine, Cairo University.

Confirmation of ovarian failure

Vaginal smear cytology: It was performed daily to ascertain ovarian failure. The cycles were considered as normal when they showed typical stages of proestrous, estrous, metestrous and diestrous, which normally last for 4-6 days [9]. Unstained vaginal smears were examined using an inverted phase-contrast microscope (Olympus, Tokyo, Japan). The presence of cornified cells in the estrous phase was used as an indicator of estrogenic activity.

Laboratory investigations: Retro-orbital blood samples were collected by capillary tubes at the Biochemistry Department, Faculty of Medicine, Cairo University.

Measuring hormonal profile for:

- Serum Estradiol (E2),
- Follicle Stimulating Hormone (FSH) and
- Lutenizing Hormone (LH), by Enzyme Linked Immuno-Sorbent Assay (Biosource, TM, ELISA Kits, USA) [10].
- This was repeated for all rats at the start of treatment as well as just before sacrifice.
- Preparation of ADSCs isolated from rats
- Isolation of ADSCs

Subcutaneous white adipose tissue was excised from the inguinal pad of fat in rat under complete aseptic conditions. The adipose tissue was resected and placed into a labeled sterile tube containing 15 ml of a phosphate buffered solution (PBS; Gibco/Invitrogen, Grand Island, New York, USA). Enzymatic digestion was performed using 0.075% collagenase II (Serva Electrophoresis GmbH, Mannheim) in Hank's Balanced Salt Solution for 60 minutes at 37 with gentle shaking. Digested tissue was filtered and centrifuged, and erythrocytes were removed by treatment with erythrocyte lysis buffer. The cells were transferred to tissue culture flasks with Dulbecco Modified Eagle Medium (DMEM, Gibco/BRL, Grand Island, New York, USA) supplemented with 10% fetal bovine serum (Gibco/BRL) and, after an attachment period of 24 hours, non-adherent cells were removed by a PBS wash. Attached cells were cultured in DMEM media supplemented with 10% fetal bovine serum FBS, 1% penicillin-streptomycin (Gibco/BRL), and 1.25 mg/L amphotericin B (Gibco/BRL), and expanded in vitro. At 80-90% confluence, cultures were washed twice with PBS and the cells were trypsinized with 0.25% trypsin in 1 mM EDTA (Gibco/BRL) for 5 min at 37. After centrifugation, cells were resuspended with serum- supplemented medium and incubated in 50 cm² culture flask (Falcon). The resulting cultures were referred to as first-passage cultures and expanded in vitro until passage four [11].

Morphological identification of ADSCs: ADSCs in culture were characterized by their adhesiveness and fusiform shape and by

detection of CD29, one of the surface markers of rat ADSCs by Flow cytometry. ADSCs differentiation into chondrocytes and osteocytes was confirmed [12]. This was done at the Biochemistry Department, Faculty of Medicine, Cairo University.

Labeling of ADSCs with PKH26 dye: ADSCs were harvested during the 4th passage and were labelled with PKH26 fluorescent linker dye [13]. ADSCs were labeled with PKH26 according to the manufacturer's recommendations (Sigma, Saint Louis, Missouri, USA). Two million units of PKH26 labelled ADSCs were loaded in a 1 ml volume sterile syringe and were injected into the tail vein of each animal. After one week and four weeks of ADSCs therapy, ovarian tissue was examined with a fluorescence microscope (Leica, Soles, and Germany) to detect and trace the cells stained with PKH26.

Histological Study

The animals were sacrificed using chloroform inhalation. Right and left ovaries from each animal were immediately dissected, fixed in 10% formol saline for 24-48 hours, dehydrated in ascending grades of alcohol, cleared in xylene and embedded in paraffin. This was performed at the Histology Department, Faculty of Medicine, Cairo University. Paraffin blocks were cut at 5 - 7µm thickness, using Leica rotator microtome (Germany).

Sections were subjected to the following stains:

Hematoxylin and Eosin stain [14].

Masson's Trichrome stain [15].

Immunohistochemical staining using the avidin-biotin peroxidase complex technique. Sections were counterstained with Meyer's hematoxylin [16] for detection of:

Proliferating Cell Nuclear Antigen (PCNA): PCNA is an auxiliary protein of DNA-polymerase enzymes, necessary for DNA synthesis and is used as a standard marker in proliferating cells [17 and 18]. PCNA antibody is a mouse monoclonal antibody PC 10 (Novocastra, Milton, Keynes, USA). PCNA positive cells show brown nuclear deposits.

Positive tissue control for PCNA: Human tonsil biopsies showed +ve immunostaining in the form of brown nuclear reaction for PCNA.

Negative control for PCNA: Additional specimens of the ovary were processed in the same sequence but the primary antibody was not added and instead, PBS was added in this step. Omission of the primary antibody gave no staining reaction.

Morphometric Study

Using a Leica Qwin 500 LTD image analysis computer system, (Cambridge, UK), the following parameters were measured. For each group, five slides of five different specimens were examined. From each slide, ten non-overlapping fields were measured.

The following parameters were measured:

- Mean number of primordial follicles. It was counted in every 5th serial section of H and E-stained sections, using the interactive measuring menu, at magnification X400.
- Mean area percent of collagen fiber content in Masson's Trichrome stained sections using the color detect menu. Collagen fibers were masked by a blue binary color to the area of the standard measuring frame, at magnification X100.

- Mean area percent of positive immunoreactivity for PCNA.

It was measured in immunostained sections using the color detect menu, in relation to a standard measuring frame, at a magnification of X400. The areas of positive immunoreactivity for PCNA were masked by a blue binary color.

Statistical Analysis

All measurements were subjected to statistical analysis using Student T test and ANOVA test using (SPSS) software version 16 Chicago USA [19].

Results

Results of laboratory investigations

Measurements of Hormone Levels (FSH, LH and Estradiol (E2) in the Studied Groups (Table 1 and Figure 1)

FSH: A significant increase was reported in the chemotherapy treated subgroups IIa and IIb, as compared to the control. FSH value presented a significant decrease in the ADSCs treated subgroups IIIa and IIIb, as compared to the chemotherapy treated group. *Thus, the highest value for FSH was recorded in subgroup IIb (after 5 weeks of chemotherapeutic treatment).*

LH: A significant increase in the chemotherapy treated subgroups IIa and IIb, was expressed as compared to the control. A reduction in the LH value was reported in the ADSCs treated group which represented a non-significant decrease in subgroup IIIa; and significant decrease in subgroup IIIb, as compared to the chemotherapy treated group. Meanwhile, a significant increase was reported in ADSCs group as compared to the control value. *Thus, the highest value for LH was recorded in subgroup IIb (after 5 weeks of chemotherapeutic treatment).*

	FSH (mIU/ml)	LH (mIU/ml)	Estradiol (pg/ml)
Gp I (control)	4.14 ± 0.32	2.83 ± 0.25	1.81 ± 0.22
Subgroup IIa	12.07 ± 1.12*# ^	9.9 ± 0.7*# ^	0.86 ± 0.05*# ^
Subgroup IIb	12.87 ± 2.25*# ^	10.83 ± 2.12*# ^	0.65 ± 0.19*# ^
Subgroup IIIa	6.31 ± 0.91 ●○	7.2 ± 0.29*●	1.27 ± 0.22 ●○
Subgroup IIIb	5.35 ± 1.56 ●○	5.7 ± 1.10*●○	1.66 ± 0.70 ●○

mIU/ml: milli international unit per milliliter
 pg/ml: picrogram per milliliter
 *Significantly different from the value of the control group at P<0.05
 # Significantly different from the value of subgroup IIIa at P<0.05
 ^ Significantly different from the value of subgroup IIIb at P<0.05
 ○ Significantly different from the value of subgroup IIa at P<0.05
 ● Significantly different from the value of subgroup IIb at P<0.05

Table 1: Mean values (±SD) of hormone levels in the studied groups.

Estradiol: A significant decrease was reported in the chemotherapy treated subgroups IIa and IIb, as compared to the control. Estradiol value presented a significant increase in the ADSCs treated subgroups IIIa and IIIb, as compared to the chemotherapy treated group. *Thus,*

the least value for Estradiol was recorded in subgroup IIb (after 5 weeks of chemotherapeutic treatment).

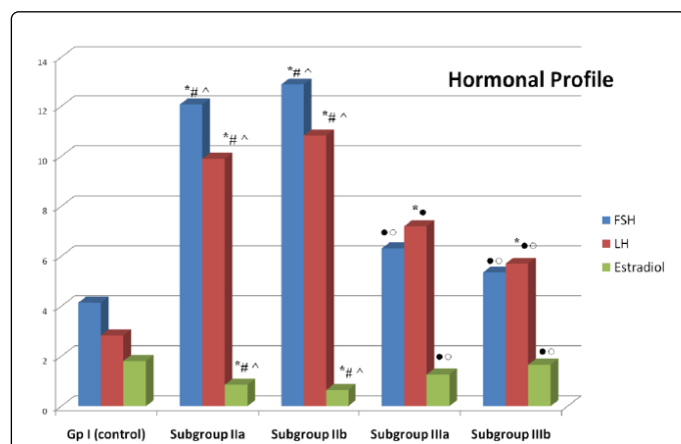


Figure 1: Mean values (\pm SD) of hormone levels in the studied groups; * Significantly different from the value of the control group at $P < 0.05$; # Significantly different from the value of subgroup IIIa at $P < 0.05$; ^ Significantly different from the value of subgroup IIIb at $P < 0.05$; o Significantly different from the value of subgroup IIa at $P < 0.05$; Significantly different from the value of subgroup IIb at $P < 0.05$.

Histological results

Hematoxylin and eosin-stained ovarian sections: No histological variations were demonstrated on examination of ovarian sections of the control subgroups. Light microscopic examination of ovarian sections of the control group (group I) showed the normal histological structure of the ovary. The surface of the ovary was covered by germinal epithelium formed of a single layer of cuboidal cells. Beneath the germinal epithelium was a thin layer of dense fibrous connective tissue (tunica albuginea). The parenchyma below the tunica albuginea was divided into two poorly demarcated zones. The outer cortex contained different types of follicles, embedded in a highly cellular compact stroma. The inner medulla contained blood and lymph vessels in loosely arranged connective tissue (Figure 2A).

Follicles in different stages of development were detected. Primordial follicles were often located immediately beneath the tunica albuginea; each consisted of a primary oocyte surrounded by a single layer of squamous epithelial cells. Unilaminar primary follicles, surrounded by a single layer of cuboidal cells and multilaminar primary follicles, surrounded by multiple layers of follicular cells, were detected. Secondary follicles were observed as well as corpora lutea. Each secondary follicle was formed of several layers of granulosa cells with multiple fluid spaces. Some atretic follicles were also observed. Cortical blood vessels were evident with a single layer of simple squamous endothelial lining (Figure 2A and 2B).

Ovarian sections of subgroup IIa showed shrunken irregular outline of the ovary with flattening of the germinal epithelium. A remarkable observation in this subgroup was massive loss of follicles and the presence of many atretic follicles. Some atretic follicles showed shrunken oocytes with dislodgement of granulosa cells. Corpora albicans, formed of dense white fibrous connective tissue, were also observed (Figure 2C and 2D).

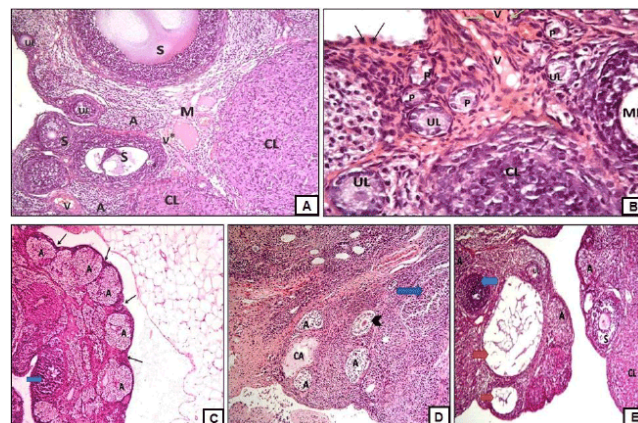


Figure 2: (A) A photomicrograph of an ovarian section of adult female albino rat of the control group (group I) showing cortex containing unilaminar primary follicles (UL), secondary follicles (S) at different stages of growth. Corpora lutea (CL) and atretic follicles (A) are also demonstrated. Note the presence of cortical blood vessel (V). The medulla (M) contains loose connective tissue rich in blood vessels (V) (H and E X100); (B) A photomicrograph of an ovarian section of adult female albino rat of the control group (group I) showing that the germinal epithelium appears formed of a single layer of cuboidal cells (black arrows). The cortex contains several primordial follicles (P), unilaminar primary follicles (UL), multilaminar primary follicle (ML) and a part of a corpus luteum (CL). Note the presence of cortical blood vessels (V) with simple squamous endothelial lining (green arrows) (H and E X400); (C) A photomicrograph of an ovarian section of adult female albino rat of subgroup IIa (1 week after chemotherapy administration) showing shrunken ovary with irregular outline (arrows) exhibiting massive loss of follicles and many atretic follicles (A). A degenerated corpus luteum (blue arrow) is observed (H and E X100); (D) A photomicrograph of an ovarian section of adult female albino rat of subgroup IIa (1 week after chemotherapy administration) showing massive loss of follicles with several atretic follicles (A). One atretic follicle shows shrunken oocyte and dislodgment of granulosa cells (arrowhead). A corpus albicans (CA) is evident in addition to a degenerated corpus luteum (blue arrow) (H and E X100); (E) A photomicrograph of an ovarian section of adult female albino rat of subgroup IIb (5 weeks after chemotherapy administration) showing irregular outline of the ovary with many atretic follicles (A) with the presence of unilaminar primary follicle (UL) and secondary follicles (S), some of which are degenerated (red arrows). A part of corpus luteum (CL) and a degenerated corpus luteum (blue arrow) are observed (H and E X100).

Ovarian sections of subgroup IIb showed irregular outline of the ovary. Ovarian cortex exhibited several atretic follicles. Some unilaminar primary, secondary follicles as well as corpora lutea were observed, but most of them were degenerated (Figure 2E).

Ovarian sections of subgroup IIIa revealed the presence of many cortical follicles at different stages of growth and development; multilaminar primary follicles, up to the mature graffian follicle stage. Mature graffian follicles were formed of primary oocytes surrounded by zona pellucida and corona radiata, covered by cumulus oophorus cells, separating the oocyte from the follicular fluid-filled cavity which

was lined by granulosa cells. The mature follicle was covered externally by theca folliculi. Several corpora lutea were also observed (Figure 3A).

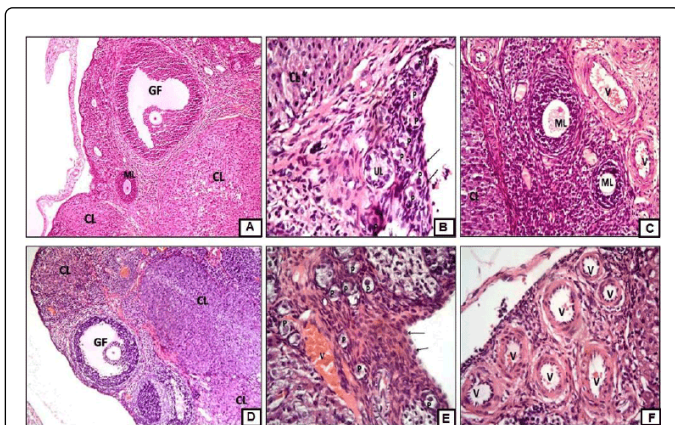


Figure 3: (A) A photomicrograph of an ovarian section of adult female albino rat of subgroup IIIa (1 week after ADSCs administration) showing a multilaminar primary follicle (ML), a mature graffian follicle (GF) as well as corpora lutea (CL) (H and E X100); (B) A photomicrograph of an ovarian section of adult female albino rat of subgroup IIIa (1 week after ADSCs administration) showing that the germinal epithelium appears formed of a single layer of cuboidal cells (arrows). Several primordial follicles (P), a unilaminar primary follicle (UL) and a part of a corpus luteum (CL) are evident (H and E X400); (C) A photomicrograph of an ovarian section of adult female albino rat of subgroup IIIa (1 week after ADSCs administration) showing multilaminar primary follicles (ML) and a part of a corpus luteum (CL) in addition to dilatation and congestion of cortical blood vessels (V) (H and E X400); (D) A photomicrograph of an ovarian section of adult female albino rat of subgroup IIIb (4 weeks after ADSCs administration) showing a mature graffian follicle (GF) and several corpora lutea (CL) (H& E X100); (E) A photomicrograph of an ovarian section of adult female albino rat of subgroup IIIb (4 weeks after ADSCs administration) showing that the germinal epithelium appears formed of a single layer of cuboidal cells (arrows). The presence of many primordial follicles (P) is noted, in addition to dilatation and congestion of cortical blood vessels (V) (H& E X400); (F) A photomicrograph of an ovarian section of adult female albino rat of subgroup IIIb (4 weeks after ADSCs administration) showing abundance of cortical blood vessels (V) which appear dilated and some of them are congested (H and E X400).

The germinal epithelium was formed of a single layer of cuboidal cells. Several primordial follicles were observed (Figure 3B). Several cortical blood vessels were noticed, where in some fields they appeared dilated and congested (Figure 3C).

Ovarian sections of subgroup IIIb revealed the presence of mature graffian follicles and several corpora lutea (Figure 3D). A remarkable abundance of primordial follicles was observed in most of the sections. The germinal epithelium was formed of a single layer of cuboidal cells (Figure 3E). Dilatation, congestion and interestingly presence of abundant cortical blood vessels were observed (Figure 3E and 3F).

Masson's trichrome (MT)-stained sections: Ovarian sections of group I (control group) showed some collagen fibers in the ovarian cortical stroma between the cortical follicles (Figure 4A). Ovarian

sections of subgroup IIa (Figure 4B) and subgroup IIb (Figure 4C) showed increased collagen fiber content in the cortical stroma between the cortical follicles and extending towards the medulla. Ovarian sections of subgroup IIIa (Figure 4D) and subgroup IIIb (Figure 4E) showed decreased collagen fiber content in the cortical stroma between the cortical follicles.

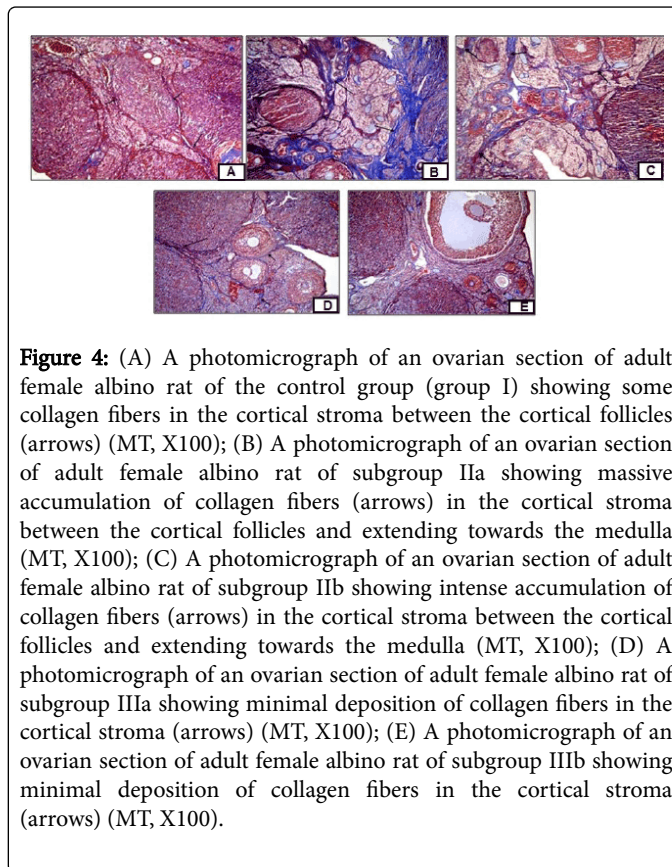


Figure 4: (A) A photomicrograph of an ovarian section of adult female albino rat of the control group (group I) showing some collagen fibers in the cortical stroma between the cortical follicles (arrows) (MT, X100); (B) A photomicrograph of an ovarian section of adult female albino rat of subgroup IIa showing massive accumulation of collagen fibers (arrows) in the cortical stroma between the cortical follicles and extending towards the medulla (MT, X100); (C) A photomicrograph of an ovarian section of adult female albino rat of subgroup IIb showing intense accumulation of collagen fibers (arrows) in the cortical stroma between the cortical follicles and extending towards the medulla (MT, X100); (D) A photomicrograph of an ovarian section of adult female albino rat of subgroup IIIa showing minimal deposition of collagen fibers in the cortical stroma (arrows) (MT, X100); (E) A photomicrograph of an ovarian section of adult female albino rat of subgroup IIIb showing minimal deposition of collagen fibers in the cortical stroma (arrows) (MT, X100).

Immunohistochemical results

Anti-PCNA stained ovarian sections: Ovarian sections of the control group immunostained for PCNA showed negative PCNA immunostaining of the surface epithelial cells. Some of the follicular cells exhibited a positive brown nuclear reaction for PCNA with negative immunostaining of the stromal cells (Figure 5A). Ovarian sections immunostained for PCNA of subgroup IIa (Figure 5B) and subgroup IIb (Figure 5C) showed negative PCNA immunostaining of the surface epithelial cells, follicular cells and stromal cells. Ovarian sections immunostained for PCNA of subgroup IIIa (Figure 5D) and subgroup IIIb (Figure 5E) showed that the surface epithelial cells had a positive brown nuclear reaction for PCNA in addition to positive immunoreactivity of follicular cells and oocyte nuclei of some primordial follicles. There was negative PCNA immunostaining of the stromal cells.

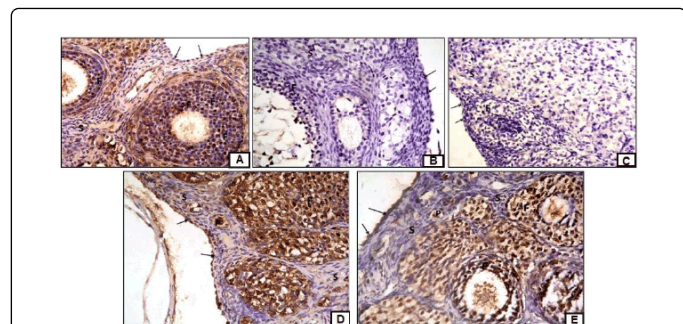


Figure 5: (A) A photomicrograph of an ovarian section of adult female albino rat of the control group (group I) showing positive PCNA immunostaining in some follicular cells (F) and negative immunostaining in the surface epithelial cells (arrows) and stromal cells (S) (PCNA immunostaining X400); (B) A photomicrograph of an ovarian section of adult female albino rat of subgroup IIa showing negative PCNA immunostaining in the surface epithelial cells (arrows), follicular cells (F) and stromal cells (S) (PCNA immunostaining X400); (C) A photomicrograph of an ovarian section of adult female albino rat of subgroup IIb showing negative PCNA immunostaining in the surface epithelial cells (arrows), follicular cells (F) and stromal cells (S) (PCNA immunostaining X400); (D) A photomicrograph of an ovarian section of adult female albino rat of subgroup IIIa showing positive PCNA immunostaining of surface epithelial cells (arrows) and follicular cells (F) as well as an oocyte of a primordial follicle (P) and negative immunostaining of the stromal cells (S) (PCNA immunostaining X400); (E) A photomicrograph of an ovarian section of adult female albino rat of subgroup IIIb showing positive PCNA immunostaining of surface epithelial cells (arrows) and follicular cells (F) as well as an oocyte of a primordial follicle (P) and negative immunostaining of the stromal cells (S) (PCNA immunostaining X400).

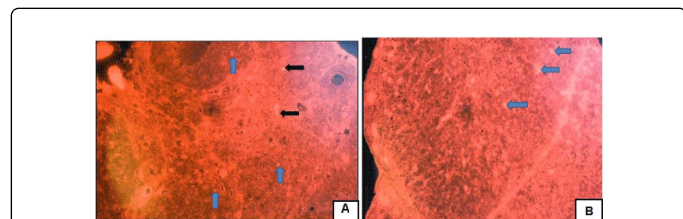


Figure 6: (A) A photomicrograph of an ovarian section of adult female albino rat of subgroup IIIa showing positive red immunofluorescent stem cells housed in the cortical stroma between the follicles (black arrows) and inside the ovarian follicles (blue arrows) (PKH26 immunofluorescence x 200); (B) A photomicrograph of an ovarian section of adult female albino rat of subgroup IIIb showing positive red immunofluorescent stem cells housed inside the ovarian follicles (blue arrows) (PKH26 immunofluorescence x 400).

Immunofluorescent results: Detection of ADSCs labeled with PKH26 fluorescent dye in ovarian tissue was done using fluorescent microscope in unstained ovarian sections. ADSCs showed strong red autofluorescence after injection into rats, confirming that these cells were seeded into ovarian tissue. Several immunostained ADSCs were

detected, housed in the cortical stroma between the ovarian follicles, and some cells were housed inside the ovarian follicles (Figure 6A and 6B).

Quantitative morphometric results: Mean number of primordial follicles (\pm SD) in the studied groups

A significant decrease was reported in both chemotherapy-treated subgroups IIa and IIb, as compared to the control. Values reported for both subgroups IIIa and IIIb, receiving ADSCs, represented a significant increase, as compared to chemotherapy-treated subgroups.

Group	Mean \pm SD
Group I (control)	25.3 \pm 8.2
Subgroup IIa	5.7 \pm 1.9*#^
Subgroup IIb	7.3 \pm 2.3*#^
Subgroup IIIa	18.9 \pm 5.3 \circ •
Subgroup IIIb	20.7 \pm 4.7 \circ •

*Significantly different from the value of the control group at $P < 0.05$

#Significantly different from the value of subgroup IIIa at $P < 0.05$

^Significantly different from the value of subgroup IIIb at $P < 0.05$

\circ Significantly different from the value of subgroup IIa at $P < 0.05$

•Significantly different from the value of subgroup IIb at $P < 0.05$

Table 2: Mean number of primordial follicles (\pm SD) in the ovarian sections of the studied groups.

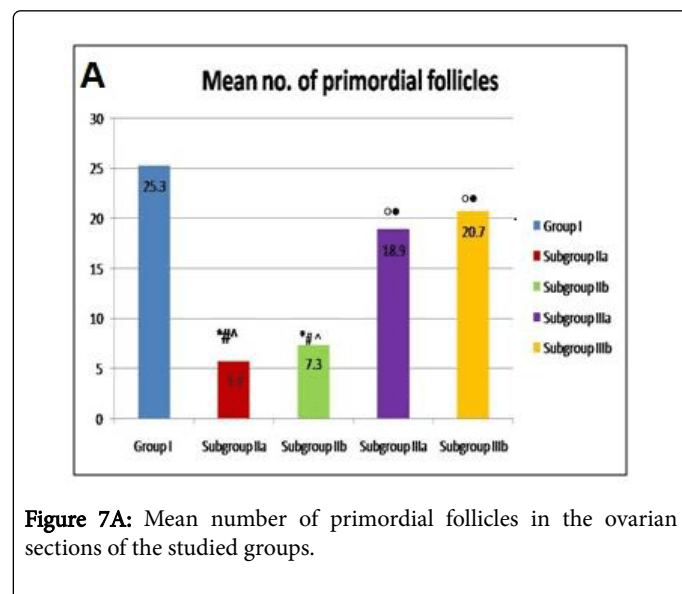


Figure 7A: Mean number of primordial follicles in the ovarian sections of the studied groups.

However, the values were not statistically significant as compared to the control. The highest value for the mean number of primordial follicles was reported with subgroup IIIb, (four weeks after ADSCs therapy), while the least value was characteristic of subgroup IIa (one week after chemotherapy) (Table 2 and Figure 7A).

Mean area percent of collagen fiber content (±SD) in the studied groups

A significant increase was reported in subgroups IIa and IIb, as compared to the control group. Values recorded for subgroups IIIa and IIIb represented a statistically significant decrease, as compared to the chemotherapy-treated subgroups. However, the values were not statistically significant as compared to the control. The highest value for the mean area % of collagen was reported with subgroup IIa (one week after chemotherapeutic treatment), while the least value was reported with subgroup IIIb, (four weeks after ADSCs therapy) (Table 3 and Figure 7B).

Group	Mean ± SD
Group I (control)	6.42 ± 1.27
Subgroup IIa	18.74 ± 5.56 ^{*#^}
Subgroup IIb	15.59 ± 3.72 ^{*#^}
Subgroup IIIa	9.79 ± 2.61 ^{°•}
Subgroup IIIb	8.30 ± 2.46 ^{°•}

Significantly different from the value of the control group at P<0.05

[#]Significantly different from the value of subgroup IIIa at P<0.05

[^]Significantly different from the value of subgroup IIIb at P<0.05

[°]Significantly different from the value of subgroup IIa at P<0.05

[•]Significantly different from the value of subgroup IIb at P<0.05

Table 3: Mean area percent of collagen fiber content (±SD) in the ovarian sections of the studied groups.

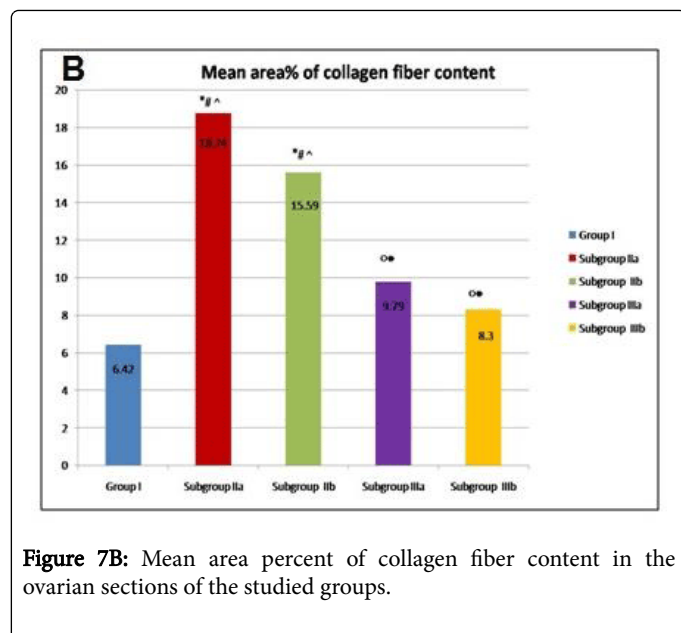


Figure 7B: Mean area percent of collagen fiber content in the ovarian sections of the studied groups.

Mean area percent of PCNA immunoreactivity (±SD) in the studied groups

A significant decrease was reported in both chemotherapy-treated subgroups IIa and subgroup IIb, as compared to the control. Values reported for both subgroups receiving ADSCs (IIIa and IIIb)

represented a significant increase, as compared to chemotherapy-treated subgroups. However, the values were not statistically significant as compared to the control. The highest value for the mean area % of PCNA immunoreactivity was reported with subgroup IIIb (four weeks after ADSCs therapy), while the lowest value was reported with subgroup IIa (one week after chemotherapeutic treatment) (Table 4 and Figure 7C).

Group	Mean ± SD
Group I (control)	4.8 ± 1.42
Subgroup IIa	0.9 ± 0.20 ^{*#^}
Subgroup IIb	2.03 ± 0.94 ^{*#^}
Subgroup IIIa	3.87 ± 0.76 ^{°•}
Subgroup IIIb	4.12 ± 1.51 ^{°•}

^{*}Significantly different from the value of the control group at P<0.05

[#]Significantly different from the value of subgroup IIIa at P<0.05

[^]Significantly different from the value of subgroup IIIb at P<0.05

[°]Significantly different from the value of subgroup IIa at P<0.05

[•]Significantly different from the value of subgroup IIb at P<0.05

Table 4: Mean area percent of PCNA immunoreactivity (±SD) in the ovarian sections of the studied groups.

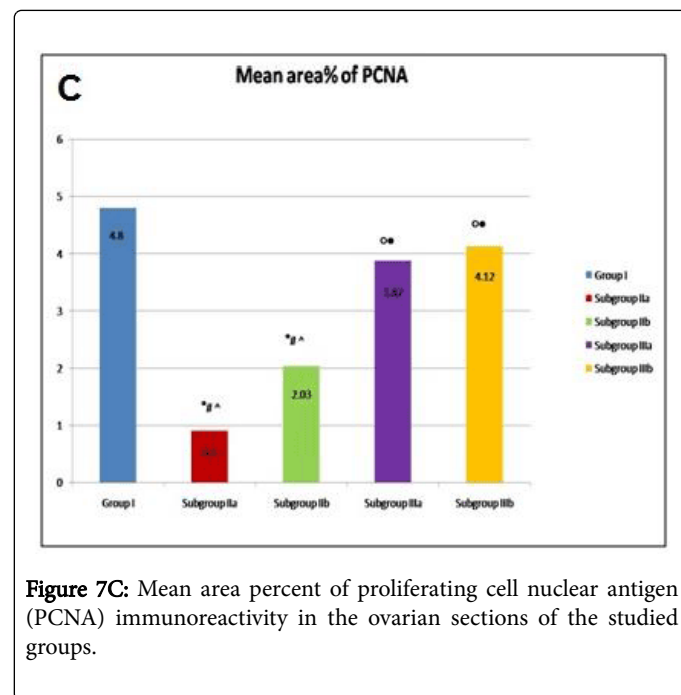


Figure 7C: Mean area percent of proliferating cell nuclear antigen (PCNA) immunoreactivity in the ovarian sections of the studied groups.

Discussion

In the present study, confirmation of ovarian failure (OF) was assessed using vaginal smears, as well as hormonal assay which showed a significant decrease in E2 level and an increase in FSH and LH levels in the chemotherapy-treated group, as compared to the control. This hormonal profile indicated the occurrence of OF. Blood tests to establish the levels of E2, FSH and LH are considered a reliable

assessment of reproductive life span of the ovaries, estimation of fertility status and the risk of premature ovarian failure (POF) [20].

There is a distinct endocrine profile seen with POE, which is partially considered to contribute to the endogenous apoptotic pathways within the ovarian follicles, thereby leading to abnormal follicular atresia. Estrogen and progesterone are mainly secreted by granulosa cells (GCs) in the ovary, which is important for stimulating proliferation as well as protecting them against apoptosis by autocrine mechanisms. Chemotherapeutic agents would damage GCs production. Therefore, the ovaries produce little to no estrogen in ovarian failure, resulting in loss of the negative feedback system to the hypothalamus and pituitary gland. Thus, the pituitary gland produces elevated levels of FSH [2].

In the present study, ovarian specimens from the chemotherapy-treated group after one week (subgroup IIa) showed shrunken irregular outline of the ovary with massive loss of follicles and the presence of many atretic follicles. After five weeks of chemotherapeutic treatment, some follicles at different stages of growth were observed, but most of them were degenerated. This implies that folliculogenesis in the present work was not restored spontaneously after recovery from chemotherapy administration. Similar results were reported by other authors who stated that chemotherapy not only destroyed the oocytes, but also affected the germ cell niche so that follicular renewal ceased after chemotherapeutic treatment [21].

Morphological results regarding follicular loss following chemotherapy in the present study went parallel with quantitative histomorphometric analysis which proved a statistically significant decrease in the mean number of primordial follicles in chemotherapy-treated group, as compared to all experimental groups.

The mechanism involved in loss of follicles after chemotherapeutic treatment is not well understood. It might result from acceleration of the natural ovarian aging process, because of a direct cytotoxic effect on oocytes and apoptotic death of a fraction of primordial follicles, impairing folliculogenesis [22]. In addition, some chemical agents may interrupt interactions between the oocytes and GCs. GCs are one of the most important follicle components; their proliferation, differentiation and apoptosis are all critical for folliculogenesis. It has been postulated that the effect of GC apoptosis on oocytes is mediated by reactive oxygen species (ROS) [23].

Vascular changes observed in the cortical blood vessels of the chemotherapy-treated group in the present study might provide an alternative explanation to follicle depletion after chemotherapy. These changes were in the form of dilatation and congestion of blood vessels. These cortical vascular changes would result in local ischemia, destroying regions of the normal ovarian cortex with subsequent loss of cortical follicles [24].

Follicular depletion encountered in the ovarian sections exposed to chemotherapy of the current work was accompanied by remarkable accumulation of collagen fiber content in the stroma of the ovary, observed in Masson's Trichrome-stained sections. Such finding was confirmed by quantitative histomorphometric analysis recording a statistically significant increase in the mean area percent of collagen fiber content in chemotherapy-treated group, as compared to all experimental groups.

This finding could be attributed to the fact that chemotherapy induced structural damage to the ovary, resulting in cortical fibrosis and loss of primordial follicles in the fibrotic cortex.

The results of the present study showed negative immunoreactivity of PCNA in follicular cells, surface epithelial cells and stromal cells in chemotherapy-treated rats, which goes parallel with the morphological findings of follicular depletion reported for the same group. This finding was confirmed by histomorphometric analysis which revealed a statistically significant decrease in the mean area % of PCNA immunoreactivity in chemotherapy-treated group, as compared to the control.

Ovarian function was improved in rats which received ADSCs therapy following chemotherapy-induced OF, as indicated by statistically significant increase in the E2 levels and significant decrease in FSH level, as compared to chemotherapy-treated group. The decrease in LH level was non-statistically significant after one week of ADSCs therapy, but was significant after four weeks of ADSCs therapy.

Going parallel with serological measurements, histological examination of ovarian sections following ADSCs administration revealed appearance of different types of follicles at various stages of growth and development; from the primordial follicles up to the mature Graafian follicle stage, as well as several corpora lutea. Concomitantly, in the current work, quantitative histomorphometric analysis confirmed these morphological findings and proved a statistically significant increase in the mean number of primordial follicles following ADSCs therapy, as compared to chemotherapy-treated group. Similar observation was reported in other studies where the total number of follicles and corpora lutea was increased following ADSCs therapy [25].

Increased chemokine concentration at the inflammation site likely directs ADSCs migration to these sites. Chemokines are released after tissue damage and ADSCs express the receptors for several chemokines such as Fibroblast growth factor-2 (FGF-2), Endothelial growth factor (EGF) and Tumor Necrosis Factor-alpha (TNF- α) [26].

ADSCs migrated to injured tissue might act by two possible mechanisms: paracrine effects and/or differentiation into cells specific to the tissue; known as transdifferentiation and serve as an integrated member of the functionally organizing adult tissue. Analysis of the soluble factors released from human ADSCs have revealed that cultured ADSCs, at relatively early passages, secrete anti-apoptotic, angiogenic and hematopoietic factors (cytokines and growth factors), such as macrophage colony-stimulating factor, hepatocyte growth factor (HGF) and vascular endothelial growth factor (VEGF) [27].

Stem cells secrete factors that act in a paracrine manner to promote angiogenesis which would provide a possible explanation for the vascular changes observed in cortical blood vessels in ovarian sections after ADSCs therapy in the present study. Meanwhile, this was reported by other authors to be a side effect of stem cells as they may cause bleeding and veno-occlusive disease [28].

The mechanism behind the recovery of ovarian activity and folliculogenesis following ADSCs therapy has not been fully elaborated, but some mechanisms such as reducing apoptosis of GCs, increasing the number of follicles and subsequent recovery of ovarian sex hormone function have been suggested in many studies [29].

The ability of ADSCs to restore ovarian tissue structure and spare ovarian follicles in the present work was further confirmed by observing decreased collagen fiber content demonstrated in Masson's Trichrome stained ovarian ADSCs-sections. Quantitative histomorphometric analysis proved a statistically significant decrease in mean area percent of collagen, as compared to chemotherapy

treated group. This could be attributed to the antifibrotic properties of MSCs which were proposed to be exerted through paracrine effects on fibroblasts [30].

The role of ADSCs in sparing follicular cells by inducing their proliferation rate was further confirmed in the current study using PCNA immunostaining, where most of the follicular cells and some surface epithelial cells stained positive with PCNA. Quantitative histomorphometric analysis of the current work proved a statistically significant increase in the mean area percent of positive PCNA immunostaining after ADSCs therapy, as compared to chemotherapy treated group.

This could be explained by the fact that, stem cells probably migrated towards the ovary, to be a source of germline stem cells capable of regenerating the population of primordial follicles and greatly preventing their apoptosis. This was reflected in a statistically significant increase in the number of primordial follicles in stem cell treated group, as compared to the chemotherapy-treated group.

PCNA immunoreactivity of the surface epithelial cells is an interesting finding in the present work. It might be hypothesized that the injected ADSCs would have migrated to the ovary and became part of the surface epithelium representing mitotically active germline stem cells [31].

The presence of such PCNA immunoreactive surface epithelial cells might also indicate occurrence of ovulation. It has been reported that the highest PCNA immunoreactivity was seen in cuboidal cells at the ovulation site the day following ovulation, during re-epithelialization of the ovulation site [32].

Positive PCNA expression in the oocytes of primordial follicles was observed in ovarian sections of ADSCs-treated rats. PCNA immunexpression in nuclei of oocytes of growing follicles is considered a marker for oocyte growth and cannot be attributed to cell division since the oocyte is arrested in the first meiotic cell division. Though arrested meiotically, the mammalian oocyte is not quiescent. It begins synthesizing nuclear RNA as it moves from the primordial to the growing phase [33].

In the current work, stromal cells of the ADSCs-treated group exhibited negative PCNA as well as Bcl-2 immunoreactivity. Previous studies of thymidine incorporation indicated that granulosa cells begin to proliferate from mitosis of the existing cells rather than recruitment from neighboring stromal cells [34]. This finding is contradictory to the results of other studies which showed that stem cells could inhibit stromal cell apoptosis through the secretion of stanniocalcin-1 and some other paracrine factors. Such paracrine effect of ADSCs implies that germ cells fail to develop unless the gonadal microenvironment is repaired by the factors released from the injected stem cells [25].

Conclusion

In this rat model of chemotherapy-induced ovarian failure, adipose-derived stem cell therapy proved to have a therapeutic potential in improving ovarian structure and function following chemotherapy.

Results in the present study provide experimental evidence ensuring the greatest effect of ADSCs after the longer duration of therapy which lasted for four weeks, although some degree of improvement was also observed after the one week, shorter duration therapy.

Recovery of ovarian structure and function by ADSCs in the current work was proved at both the laboratory level (evidenced by

measurement of serum levels of FSH, LH and Estradiol), as well as the morphological level (evidenced by improved ovarian structure and enhanced folliculogenesis).

Stimulation of proliferation by ADSCs is effective in restoration of ovarian structure and function after chemotherapeutic treatment.

Recommendations

The ability of ADSCs transplantation to rescue long-term fertility in chemotherapy-treated female rats justifies additional testing of adult stem cell-based technologies as a potential of new strategy and promising therapy for restoring fertility in human female cancer survivors, if proved to be safe and effective in humans.

Follow up studies to investigate whether offsprings of ADSCs-treated patients have congenital anomalies, developmental delay or malignant disease.

Cryopreservation of ovarian tissue in addition to the cryopreservation of embryos or oocytes for young cancer patients at risk of premature ovarian failure due to chemotherapy, prior to chemotherapeutic treatment is highly recommended.

Potential Conflict of Interest

The authors have no conflicting financial interest.

References

1. Terraciano P, Garcez T, Ayres L, Durli I, Baggio M, et al. (2014) Cell therapy for chemically induced ovarian failure in mice. *Stem Cells Int* 2014: 720753.
2. Lappi M, Borini A (2012) Fertility preservation in women after the cancer. *Curr Pharm Des* 18: 293-302.
3. Ginsburg J, Isaacs AJ, Gore MB, Havard CW (1975) Use of clomiphene and luteinizing hormone/follicle stimulating hormone-releasing hormone in investigation of ovulatory failure. *Br Med J* 3: 130-133.
4. Kode JA1, Mukherjee S, Joglekar MV, Hardikar AA (2009) Mesenchymal stem cells: immunobiology and role in immunomodulation and tissue regeneration. *Cytotherapy* 11: 377-391.
5. Takahashi K, Yamanaka S (2006) Induction of pluripotent stem cells from mouse embryonic and adult fibroblast cultures by defined factors. *Cell* 126: 663-676.
6. Mizuno H, Tobita M, Uysal AC (2012) Concise review: Adipose-derived stem cells as a novel tool for future regenerative medicine. *Stem Cells* 30: 804-810.
7. Gimble JM, Katz AJ, Bunnell BA (2007) Adipose-derived stem cells for regenerative medicine. *Circ Res* 100: 1249-1260.
8. Lai D, Wang F, Chen Y, Wang L, Wang Y, et al. (2013) Human amniotic fluid stem cells have a potential to recover ovarian function in mice with chemotherapy-induced sterility. *BMC Dev Biol* 13: 34.
9. Westwood FR (2008) The female rat reproductive cycle: a practical histological guide to staging. *Toxicol Pathol* 36: 375-384.
10. Knauff EA, Eijkemans MJ, Lambalk CB, ten Kate-Booij MJ, Hoek A, et al. (2009) Anti-Mullerian hormone, inhibin B, and antral follicle count in young women with ovarian failure. *J Clin Endocrinol Metab* 94: 786-792.
11. Huang SP, Hsu CC, Chang SC, Wang CH, Deng SC, et al. (2012) Adipose-derived stem cells seeded on acellular dermal matrix grafts enhance wound healing in a murine model of a full-thickness defect. *Ann Plast Surg* 69: 656-662.
12. Rochefort GY, Vaudin P, Bonnet N, Pages JC, Domenech J, et al. (2005) Influence of hypoxia on the domiciliation of Mesenchymal Stem Cells after infusion into rats: possibilities of targeting pulmonary artery remodeling via cells therapies?. *Respiratory Research* 6:125-137.

13. Abdel Aziz MT, Wassef MA, Rashed LA, Mhfouz S, Omar N, et al. (2011) Mesenchymal Stem Cells Therapy in Acute Renal Failure: Possible Role of Hepatocyte Growth Factor. *J Stem Cell Res Ther* 1:109-115.
14. Kiernan JA (2001) *Histologic and histochemical methods: theory and practice*. 3rd edn., Arnold publisher, London, New York & New Delhi p: 111-162.
15. Bancroft JD, Gamble M (2008) *Connective tissue stains*. In: *Theory and practice of histological techniques sixth edition*. Elsevier health Sciences, Churchill livingstone, Edinburgh, London, oxford, new York, Philadelphia, St. Louis, Sydney and Toronto: 150-157.
16. Bancroft J, Gamble M (2002) *Theory and Practice of Histological Techniques*. (5th edn) Churchill Livingstone, London, 231.
17. Kerr JB, Duckett R, Myers M, Britt KL, Mladenovska T, et al. (2006) Quantification of healthy follicles in the neonatal and adult mouse ovary: evidence for maintenance of primordial follicle supply. *Reproduction* 132: 95-109.
18. Chapman DL, Wolgemuth DJ (1994) Expression of proliferating cell nuclear antigen in mouse germ line and somatic cells suggests both proliferation-dependent and -independent modes of function. *Int J Dev Biol* 38: 491-497.
19. Emsley R, Dunn G, White IR (2010) Mediation and moderation of treatment effects in randomised controlled trials of complex interventions. *Stat Methods Med Res* 19: 237-270.
20. Torino F, Barnabei A, De Vecchis L, Appetecchia M, Strigari L, et al. (2012) Recognizing menopause in women with amenorrhea induced by cytotoxic chemotherapy for endocrine-responsive early breast cancer. *Endocr Relat Cancer* 19: R21-33.
21. Bukovsky A (2011) Ovarian stem cell niche and follicular renewal in mammals. *Anat Rec (Hoboken)* 294: 1284-1306.
22. Meiorow D, Biederman H, Anderson RA, Wallace WH (2010) Toxicity of chemotherapy and radiation on female reproduction. *Clin Obstet Gynecol* 53: 727-739.
23. Bukovsky A, Caudle MR (2012) Immunoregulation of follicular renewal, selection, POF, and menopause in vivo, vs. neo-oogenesis in vitro, POF and ovarian infertility treatment, and a clinical trial. *Reprod Biol Endocrinol* 10: 97-102.
24. Meiorow D, Dor J, Kaufman B, Shrim A, Rabinovici J, et al. (2007) Cortical fibrosis and blood-vessels damage in human ovaries exposed to chemotherapy. Potential mechanisms of ovarian injury. *Hum Reprod* 22: 1626-1633.
25. Takehara Y, Yabuuchi A, Ezoe K, Kuroda T, Yamadera R, et al. (2013) The restorative effects of adipose-derived mesenchymal stem cells on damaged ovarian function. *Lab Invest* 93: 181-193.
26. Zaragosi LE, Ailhaud G, Dani C (2006) Autocrine fibroblast growth factor 2 signaling is critical for self-renewal of human multipotent adipose-derived stem cells. *Stem Cells* 24: 2412-2419.
27. Li H, Xu Y, Fu Q, Li C (2012) Effects of multiple agents on epithelial differentiation of rabbit adipose-derived stem cells in 3D culture. *Tissue Eng Part A* 18: 1760-1770.
28. Bollard C, Krance RA and Heslop HE (2011) Hematopoietic stem cell transplantation in pediatric oncology. In: Pizzo PA, Poplack DG (eds.) *Principles and Practice of Pediatric Oncology*. (6th edn) Philadelphia: Lippincott Williams & Wilkins 16: 467-490.
29. Sun M, Wang S, Li Y, Yu L, Gu F, et al. (2013) Adipose-derived stem cells improved mouse ovary function after chemotherapy-induced ovary failure. *Stem Cell Res Ther* 4: 80.
30. Abd-Allah SH, Shalaby SM, Pasha HF, El-Shal AS, Raafat N, et al. (2013) Mechanistic action of mesenchymal stem cell injection in the treatment of chemically induced ovarian failure in rabbits. *Cytotherapy* 15: 64-75.
31. Bukovsky A, Caudle MR, Svetlikova M, Upadhyaya NB (2004) Origin of germ cells and formation of new primary follicles in adult human ovaries. *Reprod Biol Endocrinol* 2: 20.
32. Tan OL, Fleming JS (2004) Proliferating Cell Nuclear Antigen Immunoreactivity in the ovarian surface epithelium of mice of varying ages and total lifetime ovulation number following ovulation. *Biology of Reproduction*; 71: 1501-1507.
33. Muskhelishvili L, Wingard SK, Latendresse JR (2005) Proliferating cell nuclear antigen--a marker for ovarian follicle counts. *Toxicol Pathol* 33: 365-368.
34. Picut CA, Swanson CL, Scully KL, Roseman VC, Parker RF, et al. (2008) Ovarian follicle counts using proliferating cell nuclear antigen (PCNA) and semi-automated image analysis in rats. *Toxicol Pathol* 36: 674-679.